Available online at www.sciencedirect.com

SCIENCE DIRECT®

Thermochimica Acta 446 (2006) 128–134

thermochimica acta

www.elsevier.com/locate/tca

The glass transition of polymer crystals☆

Bernhard Wunderlich[a,b,*]

[a] Department of Chemistry, The University of Tennessee, Knoxville, TN 37996-1600, USA
[b] Chemical and Analytical Sciences Division, Oak Ridge National Laboratory, Oak Ridge, TN 37831-6197, USA

Abstract

The statement: “A solid is a condensed phase at a temperature below its glass transition”, is an operational definition. It leads to the corollary that for crystals to be solid, they must be below their glass transition. In this paper evidence for the usefulness of this definition is presented. It is based on the measurement of the glass transition of crystals in the presence of melting and crystallization. The experimental tool is temperature-modulated differential scanning calorimetry, TMDSC, which enables the measurement of heat capacity in the presence of irreversible latent heat of melting and crystallization. Not only is the expected change of the heat capacity during the first-order phase transition identified, but it was also discovered that in some flexible polymer crystals the glass transition of the crystal can occur at a *lower* temperature than the order/disorder process without a change in crystal structure. Typical examples for such behavior are seen in poly(oxyethylene), poly(oxytetramethylene), aliphatic nylons, and most likely also in polyesters, polyurethanes, and polymers with other functional groups, separated by longer CH_2-sequences. Such order/disorder transitions above the vitrification to a solid are well-known for the mesophases described as liquid crystals, plastic crystals, and condis crystals of small and large molecules, attesting for the universality of the operational definition.

Keywords: Glass transition of crystals; Melting transition; Macromolecule; Vibrational motion; Large-amplitude motion; Heat capacity; Mesophases

1. Introduction

The possibility of the glass transition being a property of a crystal emerged when looking for an operational definition of the type proposed by Bridgman [1] to distinguish a *solid* from a *liquid*. Certainly, there has been considerable confusion on this topic, which led in the past to the belief that only crystals are true solids and glasses are supercooled liquids. This belief is even at the present not fully abandoned. Naturally, both, glasses and crystals are quite solid at sufficiently low temperature. But while glasses always retain high, TPa s-level viscosities (10^{13} P) up to the glass transition temperature, T_g, where they turn liquid, crystals vary widely in mechanical properties. Some may have viscosities typically seen only in liquids. The dictionary definition of a *solid* goes back to the 15th century and its modern wording is [2]: “a substance that does not flow perceptibly under moderate stress, has a definite capacity for resisting forces (as compression or tension) which tend to deform it, and under ordinary conditions retains a definite size and shape.” This statement of common experience is not suitable as an operational definition because of a missing precise operation (experiment) [1]. New, thermal-analysis-based definitions evolved when trying to introduce the concepts of molecules and solids on teaching and writing about macromolecular physics [3], introductory chemistry [4], and thermal analysis [5]. In Fig. 1, an up-to-date summary of these efforts is given [6].

For glasses, it is no problem to use the glass transition temperature, T_g, as the operation to distinguish a solid from a liquid. The glass transition is defined for this purpose at the point of half-vitrification when measured by the increase in heat capacity, ΔC_p. The heat capacity is a fixed material property, and the dependence of T_g on the time-scale of the operation and its irreversible nature is by now well understood, although a detailed mathematical description has yet to be found [7].

For crystals, one is tempted to use the melting transition to separate the solid state from the mobile state. It will be shown in the body of the paper that this does not cover all situations. The two parts of the statement at the bottom of Fig. 1 can resolve this difficulty: (A) “The glass transition is a solidification without change in molecular order” or entropy. This is the

---

☆ The manuscript has been authored by a contractor of the U.S. Government under the contract No. DOE-AC05-00OR22725. Accordingly, the U.S. Government retains a non-exclusive, royalty-free license to publish or reproduce the published form of this contribution, or allow others to do so, for U.S. Government purposes.

* Tel.: +1 865 675 4532; fax: +1 865 675 4532.
E-mail address: Wunderlich@CharterTN.net.

0040-6031/$ – see front matter © 2005 Elsevier B.V. All rights reserved.
doi:10.1016/j.tca.2005.11.011

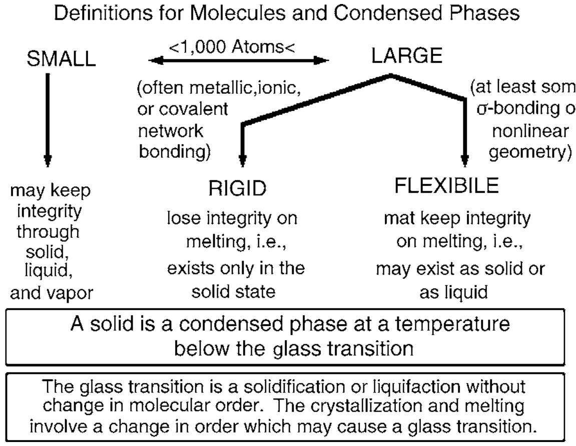

Fig. 1. Operational definitions based on thermal analysis [5].

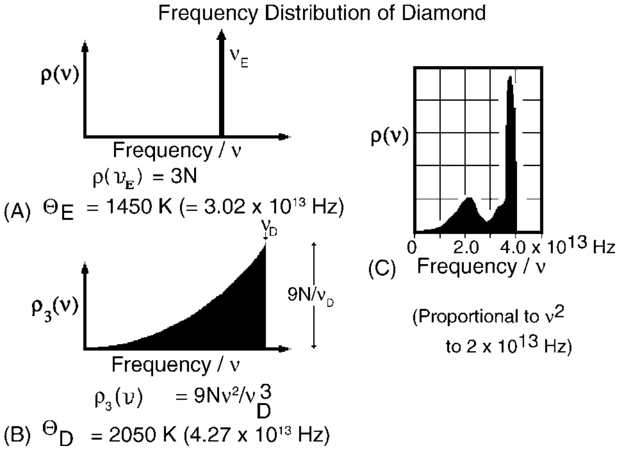

Fig. 2. Frequency distributions: (A) Einstein approximation; (B) Debye approximation; (C) normal-mode calculation [5].

generally accepted description of the glass transition measurable by thermal analysis. (B) “The crystallization and melting involve a change in order” (entropy) “which may cause a glass transition”. A glass transition, being caused by the ordering on crystallization is the novel, but obvious, suggestion at the core of the present paper. This description retains that crystallization is a first-order transition [8], linked to the change in entropy (order), measurable as a latent heat. It also suggests that the ordering, frequently connected to an increase in packing-fraction of the constituent molecules, does not always have to force a glass transition, i.e., cause a change to the solid state. At temperatures sufficiently below the phase transitions, so that all secondary relaxations due to localized, large-amplitude motions in small spatial ranges of the glass and crystals have become negligible, all solids have usually close to the same heat capacity. The jump of the heat capacity at the melting transition, thus, must be that of a glass transition, making the new formulation reasonable, useful, measurable, and all-inclusive: “A solid is a condensed phase at a temperature below its glass transition.” The possible changes in heat capacity and in entropy (latent heat) in going from the solid to the mobile state are easily determined quantitatively by thermal analysis, the operation needed for the definitions. Even mesophases, the intermediate phases between liquid and crystal, usually separated into liquid crystals, plastic crystals, and conformationally disordered (condis) crystals, can easily be included in this basic scheme of phases and transitions [6,9].

2. Characterization of a solid by its molecular motion and heat capacity

The first successful link of the macroscopic heat capacity of crystals to the microscopic molecular vibrations was given by Einstein [10]. The modeling involved the representation of the vibrational spectrum by a single frequency, the Einstein frequency, ν_E. This simplification is particularly suitable for metals, which approach a spherical force-field about each atom because of their high coordination number of 12. For the lowest temperatures where only small frequencies are excited, a better theory was developed by Debye [11]. He modeled the heat capacity with a three-dimensional continuum with a cut-off at the Debye frequency, ν_D, where the number of frequencies reaches the number of degrees of freedom. Fig. 2A and B illustrates the Einstein and Debye approximation, respectively, of the distribution of frequencies in diamond. Fig. 2C illustrates a normal-mode calculation of the full spectrum for the same crystal [12]. Although all three distributions look largely different, the figure clearly indicates the nature of the low-temperature and high-frequency approximations. The temperatures, Θ, correspond to the characteristic Einstein and Debye frequencies [$\Theta = h\nu/k$, where h is Planck’s constant and k is Boltzmann’s constant, with $h/k = 4.8 \times 10^{-11}$ K s]. They indicate the temperatures where the heat capacity reaches about 90% of its maximum value. Neither of the two approximations covers the heat capacity at all temperatures. A better model would treat the C–C-stretching vibrations as a group vibration with an approximate Einstein frequency of about 3.8×10^{-11} Hz, and the bending vibrations as a three-dimensional Debye continuum with an additional [box-averaged] frequency between 2 and 4×10^{13} Hz.

For flexible, linear macromolecules with much less symmetric force-fields, the description of the heat capacity in terms of a simple Debye or Einstein approximation of the molecular vibration spectrum is not possible [5]. Within the frame of the advanced thermal analysis system, ATHAS [13,14], it was found that the heat capacity contributions of the molecular vibrations of polymers is better assessed by separating the frequency spectrum into group and skeletal vibrations. The group vibrations are separated into approximate Einstein frequencies and, if needed, box distributions of a constant density of states over limited frequency ranges, as illustrated at the top of Fig. 3 for polyethylene. For the same chemical structures, these group frequencies change little from polymer to polymer, and even to analogous, small molecules. The group vibrations are available from Raman and infrared spectra without reference to calorimetry. In the case of polyethylene, the group vibrations consist of the C–C-stretching vibration, close to 4×10^{13} Hz, similar to the diamond in Fig. 2, and the seven C–H-bending and -stretching vibrations, leaving two skeletal vibrations to cover intra- and inter-molecular motions. These skeletal frequencies are available only by fitting experimental low-temperature heat

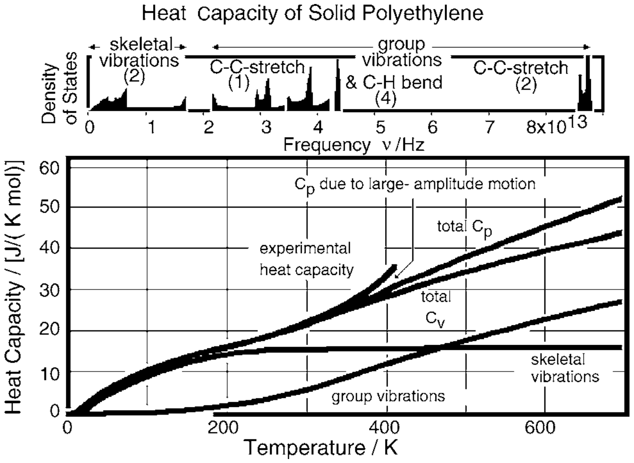

Fig. 3. Link between the frequency spectrum and heat capacity of crystalline polyethylene. The equilibrium melting temperature is 414.6 K, the entropy of fusion 10.5 J K^{-1} mol^{-1} [5].

capacities to a combination of one- and three-dimensional Debye functions, represented by Θ_1 and Θ_3, respectively [15,16].

The lower half of Fig. 3 illustrates the contributions of the skeletal and group vibrations to the heat capacity of polyethylene at constant volume, C_v. Above room temperature, the difference between C_p and C_v needs to be calculated or estimated in order to compare the calculated vibrational contributions with the experimental C_p [17,18]. Up to 200 K, practically all heat capacity contributions are due to the skeletal vibrations. At higher temperatures, increasing amounts arise from the group vibrations, but even at the 600 K, where decomposition occurs, the limiting C_p of $9 \times R = 74.8$ J K^{-1} mol^{-1} has not been attained.

Except for temperatures below about 50 K, the calculated heat capacities apply to crystalline and glassy polyethylene. The Θ-temperature for the intermolecular vibrations of the glass [Θ_3] is 80 K, while for the crystal in Fig. 3, it is 158 K. Both solids have the same intramolecular Θ_1 of 519 K.

3. Polyethylene, an example of conformational motion in the solid state

It can be seen from Fig. 3, that when approaching the melting temperature at 414.6 K, the experimental heat capacity deviates from the vibrational contributions. It was suggested earlier that this increase is either a small amount of melting, or the beginning of local, large-amplitude motions [19]. The former has recently been linked to the reversing melting of crystalline polyethylene [20]. The latter were identified in more detail when it became possible to simulate sufficiently large polyethylene crystals by molecular dynamics simulation [21]. Fig. 4 illustrates the changes of the conformation of a single chain inside a crystal starting with the ideal all-*trans* conformation at time zero. The basic C–C-bending vibrations that make up the skeletal heat capacity, the transverse, torsional, and longitudinal vibrations develop immediately after the beginning of the simulation. A collision of phonons of these three vibration types are shown to yield a kink defect after about 1.0 ps (1×10^{-12} s). This defect consists of two *gauche* conformations which keep the chain parallel, but shorten and twist the chain, as indicated.

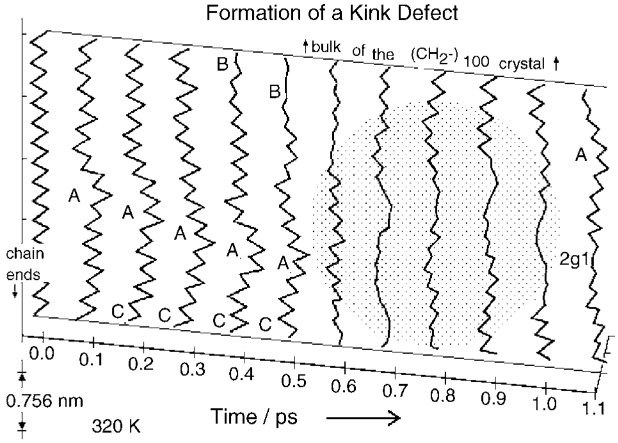

Fig. 4. Formation of a 2 g 1 kink within a computer-simulated polyethylene crystal of nine chains of 100 CH_2-groups each [21]. Displayed is the lower portion of the inner chain. The vibrations are: A, transverse; B, torsional; C, longitudinal.

The number of *gauche* conformations, as found in simulations of three cooling runs are shown in Fig. 5 [21], together with measurements of *gauche* conformations by infrared analysis of paraffins. Both methods yield analogous results, and supply proof that the increase in heat capacity beyond the vibrational contribution is due to large-amplitude motion, as is needed to introduce the kink defects. The life-time of a *gauche* conformation is in the picosecond range, allowing, despite the low concentration, each bond to go through billions of *gauche–trans* conversions per second [22]. A similar increase in heat capacity is seen at the beginning of the glass transition [13]. For both solids, these large-amplitude motions at low temperature are mainly localized and involve only short segments of the molecules. These large-amplitude motions involve increasingly larger segments and become cooperative and slow as one approaches the transitions, to speed up again when reaching the mobile phase where cooperative conformational motion becomes facile.

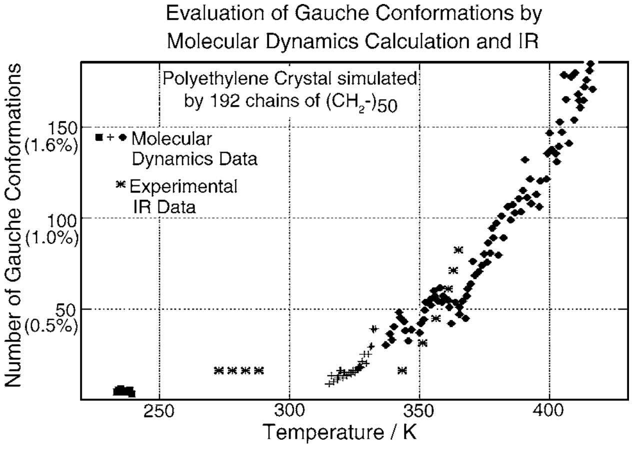

Fig. 5. Gauche concentrations as function of temperature as presented in [22].

4. Poly(oxyethylene), an example of a crystal with a glass transition

With the development of temperature-modulated differential scanning calorimetry, TMDSC, it became possible to reverse the temperature-change during a single run [23]. The modulation is either itself sinusoidal, or it is analyzed in terms of its harmonics. The reversing heat-flow-rate response to the temperature modulation is then deconvoluted by subtracting the sliding average over one modulation period, $\langle \Phi(t) \rangle$, from the instantaneous heat-flow rate, $\Phi(t)$. This analysis yields the *pseudo-isothermal response to the modulation* [24]. For reversible processes, the measured heat capacity derived from the amplitude of the pseudo-isothermal response, A_Φ, and $\langle \Phi(t) \rangle$ are identical if $\langle \Phi(t) \rangle$, which arises from the underlying, linear increase in temperature is stationary (i.e., within the error limit its value changes linearly over one modulation period). In case of the presence of additional, irreversible thermal processes, the two quantities are different. To eliminate any slow irreversible processes, which distort the deconvolution of $\Phi(t)$, a *quasi-isothermal analysis* was developed [24]. In this case, the modulation is carried out about a constant temperature, T_0, until all irreversible processes are eliminated before data are taken [$\langle \Phi(t) \rangle = 0$]. After one such run is completed, the temperature is raised or lowered to a new level. A large number of such runs cover the whole temperature-range of interest and are discussed next for the separation of latent heat of melting and crystallization from the apparent heat capacity to gain information about the glass transition in the presence of melting or crystallization.

Fig. 6 illustrates the apparent heat capacity of a crystalline, low-molar-mass poly(oxyethylene), PEO, determined by standard DSC and quasi-isothermal TMDSC [25]. At the chosen magnification, the melting of the PEO crystals seems fully irreversible. The latent heat contribution to the apparent heat capacity, however, is rather large, so that finer details need a much expanded scale, as shown in Fig. 7. Surprisingly the reversible heat capacity of Fig. 7 is much larger than the calculated vibrational contribution, evaluated as for polyethylene in Fig. 3. In fact, it approaches the level of the liquid heat capacity before the major irreversible melting starts.

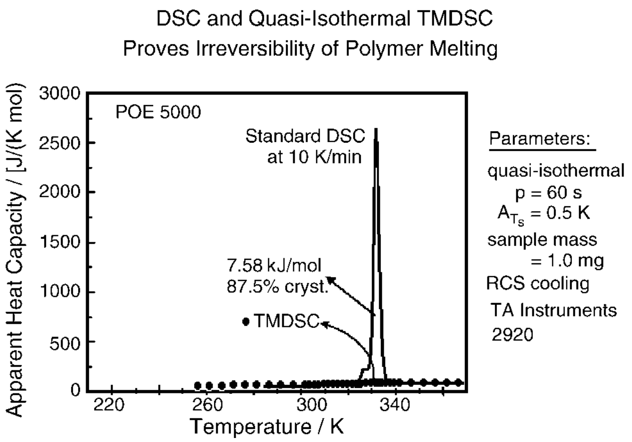

Fig. 6. Melting of POE of a molar mass of about 5000, illustrating almost complete irreversibility of melting [25].

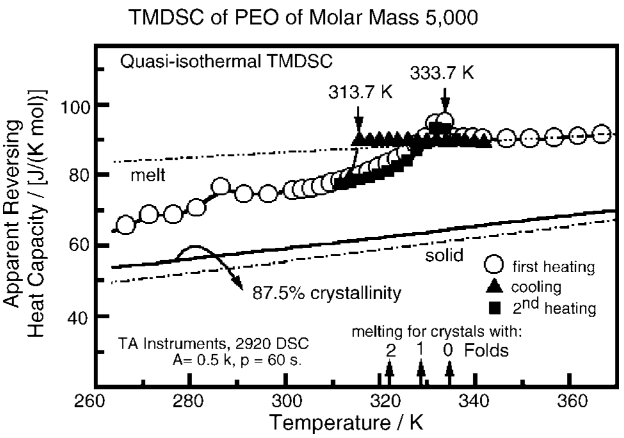

Fig. 7. Enlarged plot of the heat capacity, separated from the irreversible latent heat for the POE of Fig. 6 [25].

These early observations needed a more detailed analysis. Fig. 8 summarizes the data for PEO8000, a fraction of a molar mass of 8000 Da [26]. Quite clearly, the reversible heat capacity reaches the level of maximum conformational motion as represented by liquid PEO before major irreversible melting began. The small excess beyond the heat capacity of the liquid is a remaining reversing melting which disappears with time. At 334.1 K it settles somewhat below the heat capacity of the liquid, but far above the expected, vibrational C_p. Note, the equilibrium melting temperature of PEO8000 is 337.45 K [27]. Fig. 9 depicts the results of an extended study of quasi-isothermal TMDSC of the melting of PEOs of a wide range of molar masses. The samples range from extended-chain crystals (up to 5000 Da), to sharply folded crystals (up to 20,000 Da), to chain-folded crystals of higher molar masses.

The samples in Fig. 9 are analyzed after a quasi-isothermal series on cooling to achieve a maximum amount of annealing. Furthermore, the heat capacities are corrected for 100% crystallinity, computed from the measured heat of fusion, so that a comparison between samples of different crystallinities is possible. First, the increase of the heat capacity moves to higher

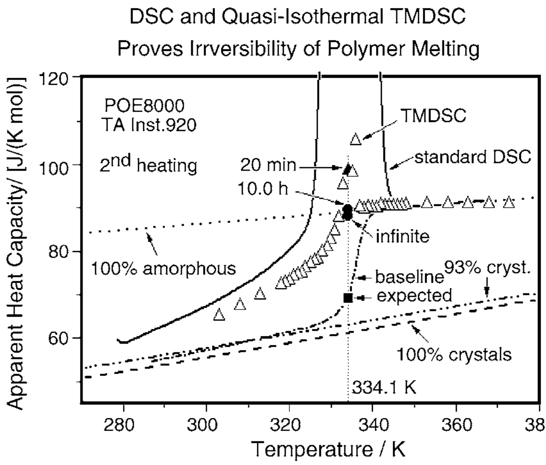

Fig. 8. Reversing C_p of POE. The filled symbols extrapolate to full reversibility with a high level of conformational mobility [26].

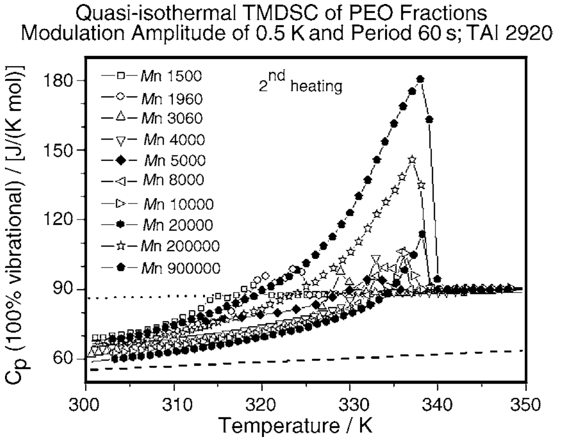

Fig. 9. Reversing melting of POE crystals with a wide range of molar masses [26].

temperature with molar mass and reaches a high-molar-mass limit at about 20,000 Da, as one sees for glass and melting transitions. Next, beyond 20,000 Da, C_p again increases at low temperature, but develops a reversible melting peak in the temperature range of irreversible melting, as has been seen for many flexible macromolecules and was explained as a surface melting of decoupled chain segments [28].

The effect of molar mass on C_p is also seen by analysis on cooling. Crystallization then occurs with the usual supercooling due to nucleation [3,29]. On completion of crystallization, the C_p matches the heating trace. Combining all these heat capacities, one can derive the approximate excess C_p for high-molar mass, as illustrated in Fig. 10. The heat capacity due to vibrational and conformational motion is represented by the black line. It has the shape expected for a glass transition, broadened by the presence of crystallinity. The transition reaches its completion before major melting is occurring, i.e., there is a temperature range of a crystal above its glass transition. The crystal shows no change in structure in this temperature range, except for a small increase in lattice spacing.

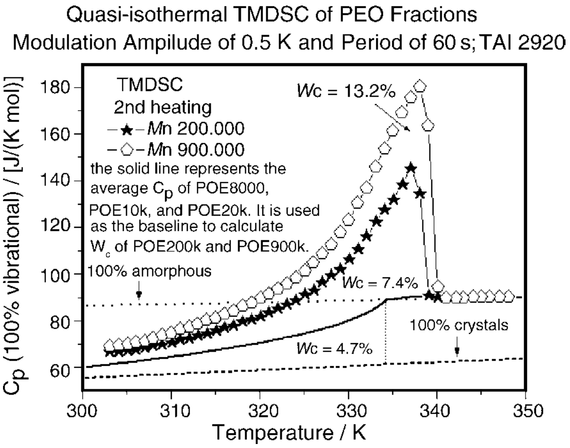

Fig. 10. Reversing melting of high-molar-mass, folded-chain crystals of POE, separated from the glass transition caused by the complete unfreezing of conformational motion below T_m [26].

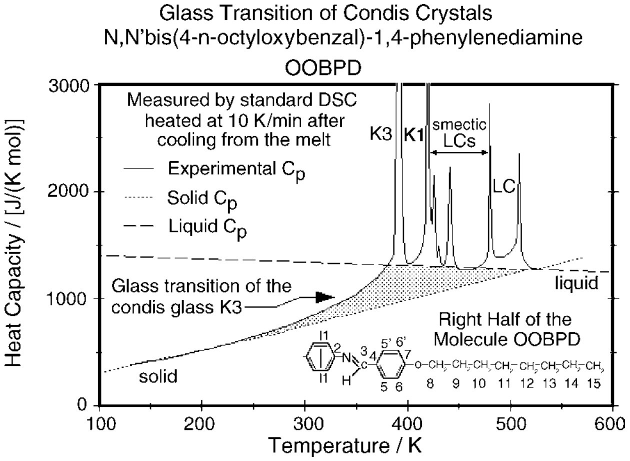

Fig. 11. Standard DSC of the liquid-crystal-forming OOBPD. The vibrational heat capacity of the solid is calculated as for polyethylene shown in Fig. 3. It is reached only below the glass transition of the condis crystal. Note also the change in order outside the transition peaks in the nematic LC-phase [31].

5. Other crystals and mesophases

A similar observation as seen in POE was also made when looking at poly(oxytetramethylene), POTM [29]. As for POEs, the POTM oligomer shows no reversible melting on quasi-isothermal TMDSC. The excess heat capacity reveals that the glass transition is practically completed when reaching the major irreversible melting peak at 300 K.

The separations of ordering and glass transitions is even more common for mesophases [30]. On cooling from the liquid, one finds first one or more first-order transitions, which produce increasing perfection of the molecular packing. The large-amplitude motion, characteristic for the mesophases, freezes at a separate glass transition when further ordering to a crystal is not possible. Fig. 11 illustrates the transitions in the small molecule OOBPD [31]. On cooling, at first, a nematic liquid crystal appears (LC). The structure of the nematic phase has only a minor amount of one-dimensional, orientational order, allowing almost free translational, liquid-like motion. On further cooling, several smectic liquid crystals result, before the K1 to K3 phases are formed. The K phases were originally thought to be crystalline, but it could more recently be proven to still have many of the parafinic C–C-bonds free to undergo conformational, large-amplitude motion, i.e., they are condis crystals [32]. After formation of K3, sufficient large-amplitude motion is possible to yield the liquid heat capacity. Only further lowering of the temperature results in a solid CD glass after the glass transition.

Fig. 12 shows a similar behavior for a partially condis-crystalline polymer. Again, the freezing to the CD glass occurs below the ordering transition and is then followed by the glass transition of the remaining amorphous polymer [33]. Both, Figs. 11 and 12 are similar to the PEO and POTM. Moreover, aliphatic nylons have been studied by DSC, X-ray, and neutron scattering. The apparent heat capacity also increases for these polymers before melting, and the conformational motion reaches the level of the liquid below the melting temperature [34,35].

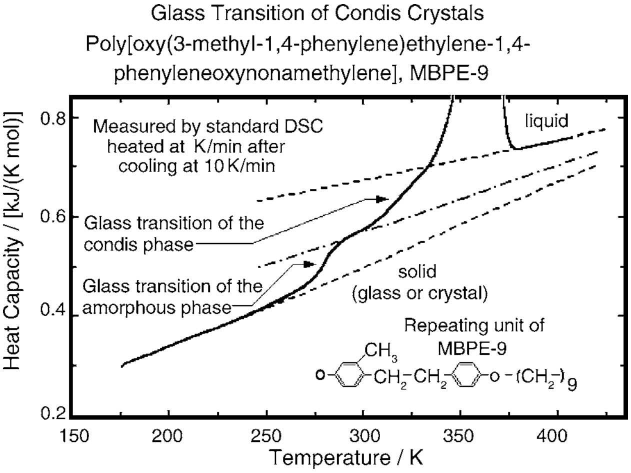

Fig. 12. Apparent heat capacity of MBPE-9, a partially ordered polymer with 43% condis phase showing its glass transition (which may be coupled to 17% rigid-amorphous phase) and a separate amorphous glass transition [33].

Similar mobility also is known for polyesters, polyurethanes, and polymers of other functional groups separated by longer CH_2-sequences.

6. Conclusions

The glass transition is introduced in Fig. 1 as the central process for the solid–liquid transition, and thermal analysis is the best-suited experiment to define the solid state, as is required for an operational definition [1]. Accepting this premise, one finds that the condensed states can be defined according to order and mobility. The thermodynamic description of the solid state can be based largely on the effect of the molecular vibrational spectrum on the heat capacity as outlined in Figs. 2 and 3. For flexible molecules, conformational motion, based largely on intramolecular hindered rotation, can begin gradually at temperatures approaching the solid-to-mobile-phase transition, detailed by the example of polyethylene in Figs. 3–5. A new research project on the apparent heat capacity of poly(oxyethylene), using mainly TMDSC, has led to the discovery that such conformational motion can reach the level of full excitation as found in the liquid state. This work is documented with Figs. 6–10 [26]. One concludes, that the glass transition and the ordering transitions may be separated without obvious changes in the crystal structure. Finally, Figs. 11 and 12 are used to show the similarity of the glass transitions of crystals to the glass transitions in mesophases to the corresponding mesophase glasses. The importance of this clarification of the solid-to-mobile-phase transition lies in the expected unique properties of crystals above their glass transition. The mobile conformational defects should cause easy deformation [21]. The polymeric crystals above their glass transition then should be able to anneal more easily, may be drawn to higher extension ratios, and lose much of the tensile modulus.

Acknowledgements

The ATHAS effort is supported by the Polymers Program of the Materials Division of the National Science Foundation (Grant #DMR-0312233) and the Division of Materials Sciences and Engineering, Office of Basic Energy Sciences, U.S. Department of Energy at Oak Ridge National Laboratory, managed and operated by UT-Battelle, LLC, for the U.S. Department of Energy, under contract No. DOE-AC05-00OR22725.

References

[1] P.W. Bridgman, The Logic of Modern Physics, MacMillan, New York 1927, reprinted by Arno Press, New York, 1980.
[2] Merriam Webster's Collegiate Dictionary, 11th ed., Merriam-Webster Inc., Springfield, MA, 2003, see also: http://www.m-w.com/.
[3] B. Wunderlich, Macromolecular physics, vols. 1–3, Academic Press, New York, London, 1973–1980.
[4] B. Wunderlich, Chemistry 2000, Workbook and Lecture Notes, Rensselaer Polytechnic Institute, Troy, NY, 1987.
[5] B. Wunderlich, Thermal Analysis of Polymeric Materials, Springer, Berlin, 2005; see also the 36-lecture computer course, Thermal Analysis of Materials, available by downloading through the internet: http://web.utk.edu/~athas, or via the European Virtual Institute for Thermal Metrology: http://www.evitherm.org/index.asp at their home page for thermal analysis and calorimetry.
[6] B. Wunderlich, A classification of molecules and transitions as recognized by thermal analysis, Thermochim. Acta 340/41 (1999) 37–52.
[7] R.J. Seyler (Ed.), Assignment of Glass Transition Temperatures Using Thermomechanical Analysis, ASTM STP 1249, American Society Testing and Materials, Philadelphia, PA, 1994.
[8] P. Ehrenfest, Phase changes in the ordinary and extended sense classified according to the corresponding singularities of the thermodynamic potential, Proc. Acad. Sci., Amsterdam 36 (Suppl. 75b) (1933) 153–157, Mitt Kammerlingh Onnes Inst., Leiden.
[9] B. Wunderlich, M. Möller, J. Grebowicz, H. Baur, Conformational motion and disorder in low and high molecular mass crystals, Springer, Berlin, 1988 (Adv. Polym. Sci., 87).
[10] A. Einstein, Die Plancksche Theorie der Strahlung und die Theorie der spezifischen Wärme, Ann. Physik. 22 (1907) 180–190 (correction, p. 800).
[11] P. Debye, Zur Theorie der spezifischen Wärme, Ann. Physik. 39 (1912) 789–839.
[12] H.M.J. Smith, The theory of the vibrations and the Raman spectrum of the diamond lattice, Phil. Trans. Act. 241 (1948) 105.
[13] B. Wunderlich, The heat capacity of polymers, Thermochim. Acta 300 (1997) 43–65.
[14] B. Wunderlich, The Athas data base on heat capacities of polymers, Pure Appl. Chem. 67 (1995) 1019–1026; see also B. Wunderlich, Heat capacity of polymers, in: S.Z.D. Cheng (Ed.), Handbook of Thermal Analysis and Calorimetry, vol. III, Applications to Polymers and Plastics, Elsevier Science, Amsterdam, 2002, pp. 1–47. For a collection of critically analyzed data, see the website: http://web.utk.edu/~athas.
[15] V.V. Tarasov, Theory of the heat capacity of chain and layer structures, Zh. Fiz. Khim. 24 (1950) 111–128.
[16] M. Pyda, M. Bartkowiak, B. Wunderlich, Computation of heat capacities of solids using a general Tarasov equation, J. Thermal Anal. Calorim. 52 (1998) 631–656.
[17] R. Pan, M. Varma, B. Wunderlich, On the C_p to C_v conversion for solid linear macromolecules II, J. Thermal Anal. 35 (1989) 955–966.
[18] J. Grebowicz, B. Wunderlich, On the C_p to C_v conversion of solid linear macromolecules, J. Thermal Anal. 30 (1985) 229–236.
[19] B. Wunderlich, H. Baur, Heat capacities of linear high polymers, Fortschr. Hochpolymeren Forsch. [Adv. Polymer Sci.] 7 (1970) 151–368.
[20] B. Wunderlich, The contributions of MDSC to the understanding of the thermodynamics of polymers, J. Therm. Anal. Calorim. (2005), in press.
[21] B.G. Sumpter, D.W. Noid, G.L. Liang, B. Wunderlich, Atomistic dynamics of macromolecular crystals, Adv. Polym. Sci. 116 (1994) 27–72 (vol.

on Atomistic Modeling of Physical Properties of Polymers, U. Suter, L. Monnerie, (Eds.)).

[22] B. Wunderlich, M. Pyda, J. Pak, R. Androsch, Measurement of heat capacity to gain information about time scales of molecular motion from pico to megaseconds, Thermochim. Acta 377 (2001) 9–33.

[23] M. Reading, D. Elliott, V. Hill, Some aspects of the theory and practice of modulated differential scanning calorimetry, in: Proceedings of the 21st NATAS Conference, vol. 21, Atlanta, GA, 1992, pp. 145–150.

[24] B. Wunderlich, Y. Jin, A. Boller, Mathematical description of differential scanning calorimetry based on periodic temperature modulation, Thermochim. Acta 238 (1994) 277–293.

[25] K. Ishikiriyama, B. Wunderlich, Melting of poly(oxyethylene) analyzed by temperature-modulated calorimetry, Macromolecules 30 (1997) 4126–4131.

[26] W. Qiu, M. Pyda, E. Nowak-Pyda, A. Habenschuss, B. Wunderlich, Reversibility between glass and melting transitions of poly(oxyethylene), Macromolecules 38 (2005) 8454–8567.

[27] S.Z.D Cheng, B. Wunderlich, Molecular segregation and nucleation of poly(ethylene oxide) crystallized from the melt. I. Calorimetric study, J. Polym. Sci., Part B, Polym. Phys. 24 (1986) 577–594.

[28] B. Wunderlich, Reversible crystallization and the rigid amorphous phase in semicrystalline macromolecules, Prog. Polym. Sci. 28 (2003) 383–450.

[29] J. Pak, M. Pyda, B. Wunderlich, Temperature-modulated calorimetry of hexacontane and oligomer fractions of poly(oxyethylene) and poly(oxytetramethylene), Thermochim. Acta 396 (2003) 43–56.

[30] B. Wunderlich, J. Grebowicz, Thermotropic mesophases and mesophase transitions of linear, flexible macromolecules, Adv. Polym. Sci. 60/61 (1984) 1–59.

[31] J. Cheng, Y. Jin, G. Liang, B. Wunderlich, H.G. Wiedemann, Condis crystals of small molecules. V. Solid state ^{13}C NMR and thermal properties of *N*,*N*′-*bis*[4-*n*-octyloxybenzal]-1,4-phenylenediamine [OOBPD], Mol. Cryst., Liq. Cryst. 213 (1992) 237–258.

[32] J. Cheng, W. Chen, Y. Jin, B. Wunderlich, Condis crystals of small molecules. VI. The differences between smectic and condis phases, evaluated by a solid state ^{13}C NMR study of *N*,*N*′-*bis*[4-*n*-octyloxbenzal]-1,4-phenylenediamine [OOBPD], Mol. Cryst. Liq. Cryst. 241 (1994) 299–314.

[33] Y. Jin, J. Cheng, B. Wunderlich, S.Z.D. Cheng, M.A. Yandrasits, Thermodynamic functions of thermotropic polyethers based on the semiflexible mesogen 1-[4-hydroxyphenyl]-2-[2-methyl-4-hydroxyphenyl]ethane, Polym. Adv. Technol. 5 (1994) 785–795.

[34] A. Xenopoulos, B. Wunderlich, A.H. Narten, Proton motion in aliphatic nylons from neutron scattering, Macromolecules 26 (1993) 1576–1581.

[35] A. Xenopoulos, B. Wunderlich, Conformational motion and disorder in aliphatic nylons, the case of nylon 6.6, Colloids Polym. Sci. 269 (1991) 375–391.